

## INVESTIGATIONS AND MIMICRY OF THE OPTICAL PROPERTIES OF BUTTERFLY WINGS

CHRISTOPHER J. SUMMERS<sup>\*,§</sup>, DAVY P. GAILLOT<sup>\*</sup>,  
MATIJA CRNE<sup>†</sup>, JOHN BLAIR<sup>\*</sup>, JUNG O. PARK<sup>†</sup>,  
MOHAN SRINIVASARAO<sup>†</sup>, OLIVIER DEPARIS<sup>‡</sup>,  
VICTORIA WELCH<sup>‡</sup> and JEAN-POL VIGNERON<sup>‡</sup>

<sup>\*</sup>*School of Materials Science and Engineering,  
Georgia Institute of Technology, Atlanta,  
Georgia 30332-0245, USA*

<sup>†</sup>*School of Polymer, Textile, and Fiber Engineering,  
Georgia Institute of Technology, Atlanta,  
Georgia 30332-0245, USA*

<sup>‡</sup>*Laboratoire de Physique du Solide, Facultés Universitaires  
Notre-Dame de la Paix, B-5000 Namur, Belgium*

<sup>§</sup>*chris.summers@mse.gatech.edu*

Received 22 August 2010

Structural color in Nature has been observed in plants, insects and birds, and has led to a strong interest in these phenomena and a desire to understand the mechanisms responsible. Of particular interest are the optical properties of butterflies. In this paper, we review three investigations inspired by the unique optical properties exhibited in a variety of butterfly wings. In the first investigation, conformal atomic layer depositions (ALDs) were used to exploit biologically defined 2D photonic crystal (PC) templates of *Papilio blumei* with the purpose of increasing the understanding of the optical effects of naturally formed dielectric architectures, and of exploring any novel optical effects. In the second study, it was demonstrated that faithful mimicry of *Papilio palinurus* can be achieved by physical fabrication methods through using breath figures to provide templates and ALD routines to enable optical properties. Finally, knowledge of the optical structure properties of the *Priniceps nireus* butterfly has resulted in bioinspired designs to enhanced scintillator designs for radiation detection.

*Keywords:* Atomic layer deposition; colloidal photonic crystal; bioinspired structures, butterfly.

### 1. Introduction

In the search for multifunctional materials, Nature provides many interesting examples and lessons. The wings of Lepidoptera, an order of the class Insecta, are an excellent example, in that they are aerodynamically shaped, structurally strong, lightweight, and endowed with many fluidic, thermal and optical properties. Recently the latter effects have received considerable attention, and have been shown to exhibit a wide range of reflective, absorptive and emissive properties

that are related to subtle nanostructures and material property variations.<sup>1</sup> In fact, Nature exhibits an astonishing variety of optical effects using very-low-index-contrast materials,<sup>1,2</sup> and a deeper understanding of these phenomena can impact future developments in nanophotonics. We have therefore investigated a variety of these phenomena and here we report studies of three different butterfly wing sections.

## 2. Optical Properties of *Papilio blumei* Infiltrated Scales

In this study, we focused on a tropical butterfly species commonly found in Indonesia: *Papilio blumei* [Fig. 1(a)], whose forewing and tip tailwing sections exhibit strong green and blue iridescence, respectively. This color stimulus phenomenon<sup>3</sup> is typical of species presenting a concavity variation of scales (*Urania* type or class II), such as the *P. palinurus* and *P. ulysses* butterflies.<sup>4</sup> Indeed, low-magnification secondary electron microscopy (SEM) images reveal that the scales of the *P. blumei* consist of an ordered array of concavities or bowls, 5–10  $\mu\text{m}$  in diameter, as shown

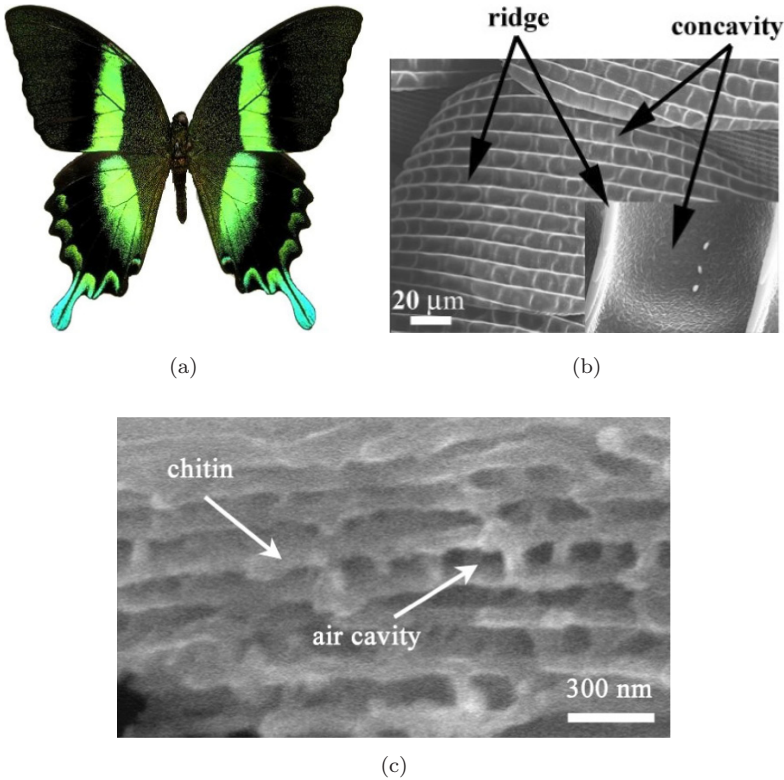


Fig. 1. (a) The Indonesian *Papilio blumei* butterfly: the wings present green iridescence bands, whereas the tail color is blue. (b) SEM image of the scale, showing concavity/ridge structure and concavities (inset). (c) Cross-section of the concavity region, revealing a thin film stack which consists of eight air layers/nine chitin layers, producing a Bragg diffraction peak at  $\sim 525$  nm.

in Fig. 1(b). Additionally, the SEM images indicate that the scales are completely sealed, in contrast to class I species (*Morpho* type).<sup>5</sup> In 1999, Tada *et al.* investigated and modeled the optical properties of *P. blumei* and observed that each scale is composed of nanometer-sized rectangular air chambers separated by transverse and longitudinal chitin laminae (refractive index  $n \sim 1.6$ ), as confirmed by SEM imaging of the internal architecture [Fig. 1(c)]. Subsequently, Vukusic *et al.* modeled the influence of wing curvature on the optical response and highlighted more complex effects whereby light was doubly reflected off opposite walls of a concavity, resulting in an ingenious coloration and polarization mechanism.<sup>6</sup>

In this work, we have deliberately perturbed the optical properties by using low-temperature ALD depositions of optically transparent TiO<sub>2</sub> layers on the biological template and studied the dependence of the resulting optical properties on dielectric structure. This has involved exterior coatings and infiltration through surface microcracks.

The depositions were performed on 5 mm × 5 mm samples in a custom-built ALD reactor designed for the deposition of TiO<sub>2</sub> and Al<sub>2</sub>O<sub>3</sub>. Conformal and progressive deposition of amorphous TiO<sub>2</sub> was performed by low-temperature ALD at 100°C,<sup>7</sup> and a total thickness of 50 nm was achieved by sequential 10 nm deposits of TiO<sub>2</sub> at a growth rate of 0.075 nm/cycle. Between each ALD run, the dependence of the normal-incidence specular reflectance was measured between 400 and 1100 nm and the change in architecture monitored by SEM analysis to determine the TiO<sub>2</sub> thickness, and assess the surface roughness and degree of infiltration of the air/chitin stack. To minimize effects resulting from the long-range curvature of the scale and eliminate undesired optical perturbations from adjacent scales, a 40X objective was used to collect light from a spot size of  $\sim 50 \mu\text{m}$ . This approach was essential for assessing the optical properties of the scales for normal incidence. Also, all spectra were normalized to the spectrum obtained from aluminum-coated glass. Typically, the probed surface encompasses  $\sim 10$  concavities with a fractional reflectivity or surface contribution to the interference effect estimated at 0.36, as also reported by Tada *et al.*<sup>5</sup> A CCD camera, mounted on a 4.5X binocular microscope, was used to record the long-range color uniformity of bare and coated samples.

Simulations of the reflectance of uncoated and conformally coated scales were calculated using the TMM technique based on the 2D structural model developed by Tada,<sup>5</sup> in which the structural parameters were determined from high-magnification SEM images of the scale cross-section [Fig. 1(c)]. Layers containing air cavities were replaced by homogeneous layers using the effective index approximation. This allowed the structure to be modeled as a 1D photonic crystal thin film interference stack [Fig. 2(a)] of eight air–chitin layers (thickness  $d_2 = 90 \text{ nm}$ ) and nine chitin layers (thickness  $d_1 = 100 \text{ nm}$ ), where the air cavities have transverse length  $D = 170 \text{ nm}$ , separated by distance  $d = 100 \text{ nm}$ . This gives an air-filling fraction,  $f_{\text{air}} (= d/D)$ , of  $\sim 59\%$ . A complex refractive index ( $n + ik$ ) was used for chitin ( $n = 1.58, k = 0.06$ ), because it was necessary to include the effect of absorption ( $k$ ) which reduced the intensity of the reflectance peaks and oscillations in order

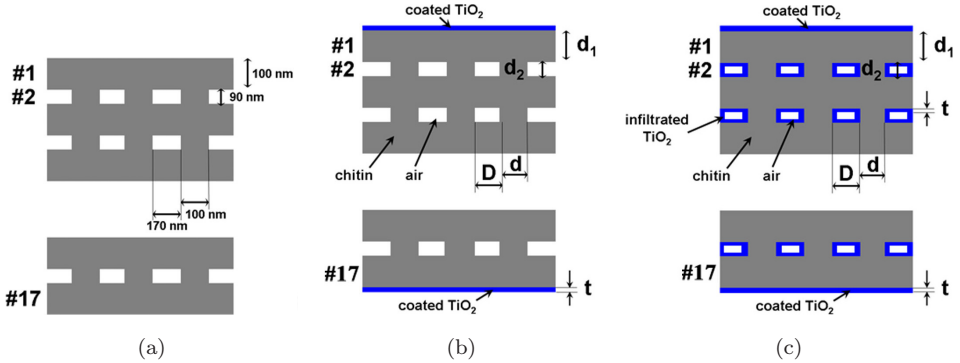


Fig. 2. (a) 2D model used for the simulations of the uncoated *P. blumei* scale. The structural parameters were determined from transverse SEM cross-sections such as that shown in Fig. 1(c). (b) 2D model used to simulate the hermetic *P. blumei* scale coated externally by ALD.  $\text{TiO}_2$  ( $n_{\text{TiO}_2} = 2.31$ ) is deposited only as the top and the bottom of the scale. (c) 2D model used to simulate the fractured *P. blumei* scale internally and externally coated by ALD.  $\text{TiO}_2$  is deposited at the top and the bottom of the scale, and also on the interior of the chitin walls.

to fit the experimental measurements. The models used for simulating the optical properties of the externally and externally/internally ALD-coated samples are shown in Figs. 2(b) and 2(c), respectively. For these calculations the dispersion of amorphous  $\text{TiO}_2$  was included and for all simulations the reflectance spectra were averaged over incidence angles between  $-60^\circ$  and  $+60^\circ$  to account for the curvature of the concavities.

Figures 3(a) and 3(b) depict, respectively, the measured and the simulated reflectance spectrum of the uncoated sample between 400 and 1100 nm. The measured spectrum is dominated by a well-defined peak at 524 nm and is well-fitted by the simulations assuming optical interference resulting from the interaction of the incident light with the air/chitin stack. The four weak maxima observed at longer wavelengths (652, 742, 850 and 1054 nm) make a minimal contribution to the far-field green iridescence. The external surfaces of the scales were then sequentially coated in 10 nm steps with amorphous layers of  $\text{TiO}_2$  deposited by low-temperature ALD to a total thickness of 50 nm. Figure 3(a) shows that, apart from a slight shift to longer wavelengths, there was little change in the main peak, but that the longer-wavelength oscillations progressively increased in magnitude and showed only slight shifts in the wavelength position. Theoretically the model explains the increase in intensity but, in contrast to the experimental data, it predicted a shift of all peaks to longer wavelengths.

The measured and simulated patterns display spectral characteristics very typical of those observed from Fabry–Perot optical cavities. Hence, in the organic/inorganic sandwich structure studied, the high-index bottom and top  $\text{TiO}_2$  layers, which behave as reflective mirrors, are responsible for the formation of additional reflected modes. More importantly, the results demonstrate that the precise control over the mirror thickness by ALD enables the finesse or quality factor

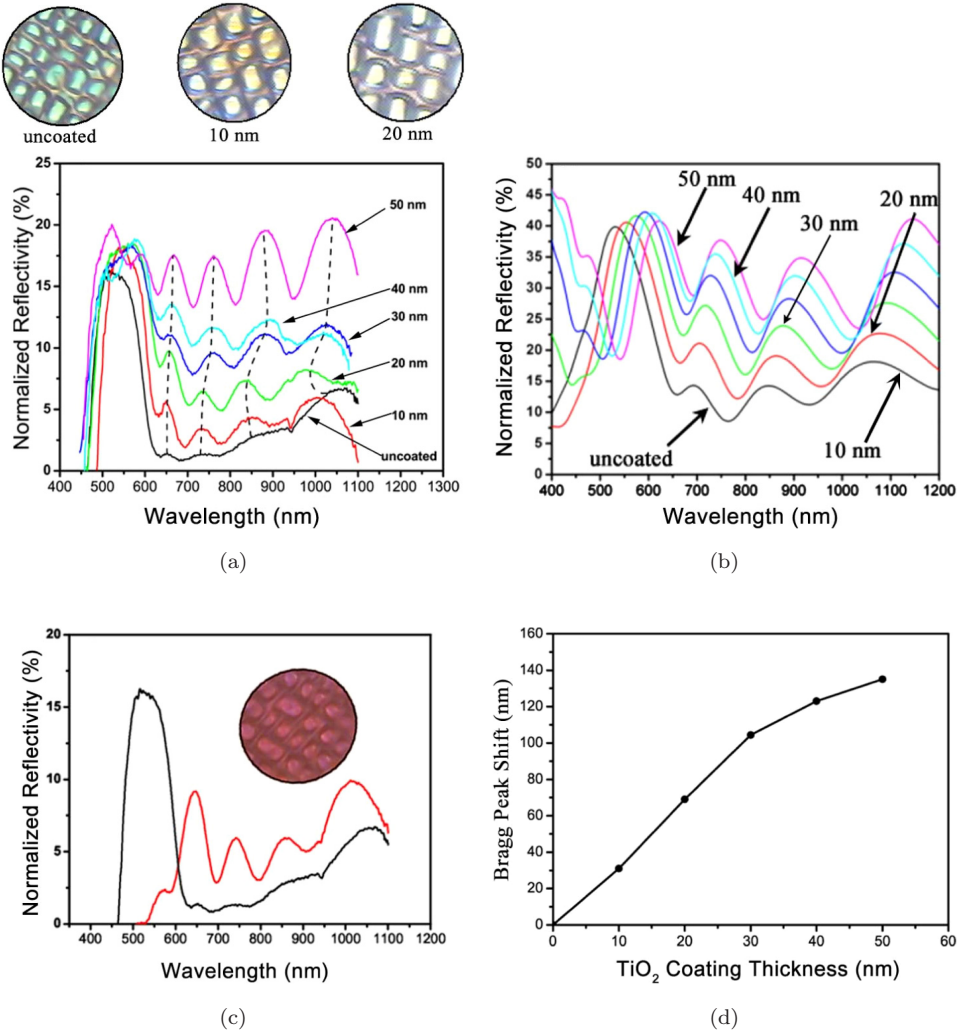


Fig. 3. Comparison between measured (a) and simulated (b) reflectance spectra of an uncoated scale of a *P. blumei* butterfly that is progressively coated by 10-nm-thick TiO<sub>2</sub> coatings up to 50 nm. A  $\sim 524$  nm peak is observed and predicted, and is responsible for the green color of the wing. CCD images of iridescent concavities taken at 40X magnification are shown. (c) Measured reflectance spectra of the uncoated (black) and 10 nm infiltrated scale (red). The inset shows the CCD image of infiltrated iridescent concavities. (d) Simulated Bragg peak shift for TiO<sub>2</sub> coating thickness values ranging from 0 to 50 nm.

of the hybrid etalon to be finely tuned and enhanced with subsequent chromatic adjustments. For example, to the naked eye the initial green color was progressively attenuated to paler nuances [Fig. 3(a)]. This optical effect can be explained by the fact that the human eye displays a tristimulus response to primary colors (blue, green and red) and averages a multicolor spectrum into a monochromatic color.

The chromaticity is strongly dependent on the intensity and frequency of the spectral components and can be positioned on a 2D color map as defined by the CIE 1931 convention.<sup>8</sup>

By selecting samples with small surface microcracks and fissures, the gas precursors diffuse into the template and thin dielectric layers are conformally deposited both over the scale body and onto the interior of the chitin walls, as depicted in Fig. 2(c), such that the scales become externally and internally coated. Figure 4 depicts the high-index inverted  $\text{TiO}_2$  skeleton remaining after burning out the chitin template. The scales mostly preserved their original shape but some long-range order was lost, although this figure shows that homogeneous infiltration was achieved and that the air cavities formed a fully interconnected network. Visually the scales look white, as confirmed by the broad reflectance spectrum measured from these samples [Fig. 4(b)]. This experimental finding can be used to improve the present model (in which separated air cavities were assumed) or to extend it to a 3D photonic crystal model, as recently reported in the case of an iridescent weevil.<sup>9</sup> The optical properties of the scales, largely discussed in Ref. 10, are shown to behave as low-index porous networks conformally infiltrated by a high-index material similar to synthetic opals<sup>7, 11, 12</sup> and holographically defined templates.<sup>13</sup> Indeed, Fig. 3(c) presents the spectra measured for the uncoated and 10 nm coated sample, whereas Fig. 3(d) presents the simulated (from uncoated to 50 nm) Bragg peak shift with increasing layer thickness. The large 122 nm shift in the central peak can be directly attributed to the reduction in the filling fraction of air from  $\sim 59$  to  $\sim 37\%$ , and the subsequent increase in the effective index of the infiltrated stack, as can be inferred from Fig. 2(c).

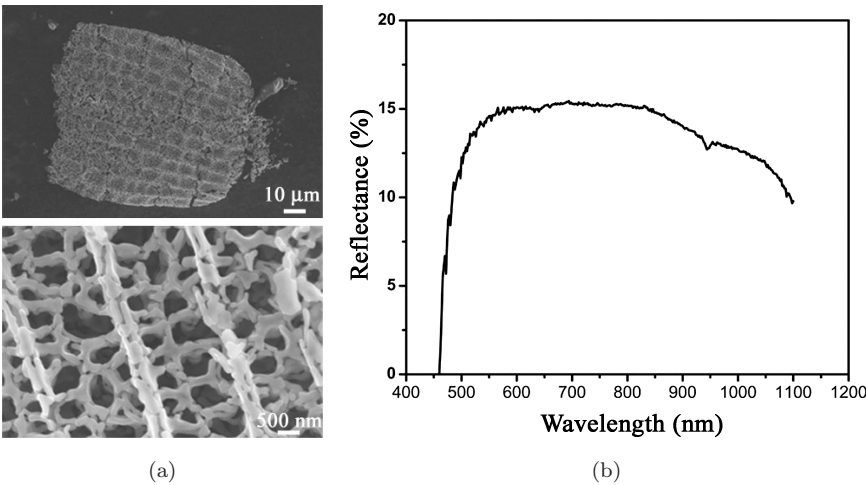


Fig. 4. (a) High-index inverted  $\text{TiO}_2$  skeleton remaining after heating to burn out the chitin template. The scales mostly preserved their original shape but some long-range order was lost. Visually the scales appear very white, as confirmed by the broad reflectance spectrum measured from these samples (b).

### 3. Mimicry of *Papilio palinurus* Scale Architecture

The unique coloration of the *Papilio palinurus* butterfly also depends on optical interference effects produced by a chitin/air multilayer stack. However, in this structure the interference stack lines a highly curved concavity that forms an open hemisphere, as illustrated in Fig. 5(a) (after Vukusic *et al.*<sup>6</sup>) For this geometry the component of white light reflected from the center of each cavity is solely determined by the properties of the 11-chitin-layer and 10-air-layer interference stack, and in this case it is yellow. In contrast, light incident on the side of the bowl strikes the interference stack obliquely and those rays incident at  $45^\circ$  are reflected to the opposite side of the bowl and then reflected again by  $45^\circ$  to exit the concavity in the direction of the incoming white light. This double reflection results in a strong linear polarization (and polarization rotation) and the reflection of only blue light due to the properties of the interference film [Fig. 5(b)]. However, the additive properties of the human eye record the color green — because, as mentioned previously, the human eye averages a multicolor spectrum into a monochromatic color which can be positioned on a 2D CIE color map.<sup>8</sup>

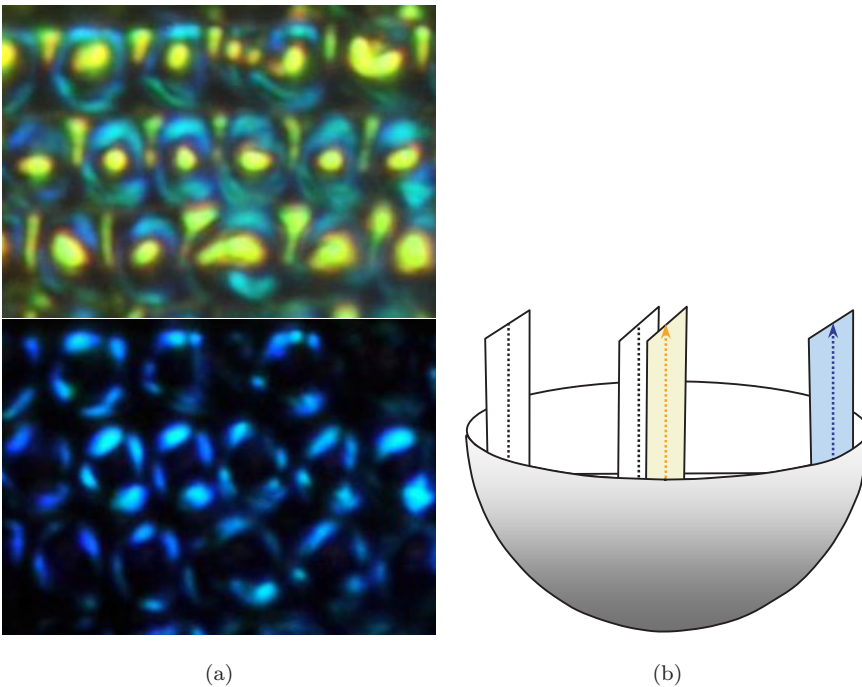


Fig. 5. Structure and optical properties of *P. palinurus*. Wavelengths of reflected light controlled by microcavity thin film and retroreflection produce a color variation across each concave surface modulation. Thus, flat regions in each concavity appear yellow and inclined sides of each concavity appear blue (double reflection). The human eye cannot resolve these small features and sees green (the same principle as for color television, pointillistic painting white LEDs).

We have emulated the properties of *P. palinurus* by using breath figure self-assembly to form a template of hexagonal spheres (a 1D opal structure) for the subsequent growth of an interference stack using conformal depositions of  $\text{TiO}_2$  and  $\text{Al}_2\text{O}_3$  by ALD. To form the template, humid air is flowed across a polymer solution in a volatile solvent, and the evaporation of the solvent cools the solution, thus promoting the condensation of monodispersed water spheres. These water droplets pack into a hexagonal lattice around which the polymer solidifies, and upon evaporation of the water an inverse opal structure is left behind in the polymer film. (Note: With this technique a monodispersion of water spheres whose diameter is determined by the vapor pressure, temperature and flow rate of the humid air can be produced with diameters ranging from 50 nm to 20  $\mu\text{m}$ ). By cleaving this structure along a (100) plane, an array of hexagonal microbowls was formed. As can be seen from Fig. 6(a), the base template of the structure formed by breath figure assembly compares very favorably with the image shown for the real butterfly in Fig. 5(a). Using ALD a conformal multilayered thin film consisting of five alternate layers of  $\text{Al}_2\text{O}_3$  and  $\text{TiO}_2$ , each 20 nm thick, was then deposited, where the thickness of each material and the number of layers were designed to produce a broad reflection at 540 nm — in the yellow region of the spectrum. In the design of the thin film, careful attention was paid to minimizing the number and thickness of the layers so as to produce these effects with a thin layer that would not interfere with the nanobowl structure. Optical reflectance measurements showed a strong but broad spectrum centered on the design wavelength at 540 nm with a reflectance of 25% as compared to an Al mirror.

Figure 6(b) shows an optical micrograph of the ALD-coated polymer microbowl array in reflection. The center of each bowl reflects bright yellow, whose spectra are centered at 550 nm. Figure 6(c) shows an optical micrograph taken with crossed polarizers from which a blue–green reflection was observed around edges of each bowl. (Note: The red reflections between bowls are due to imperfect edges of the peeled microbowls). Thus, to first order, both the structure and the optical color

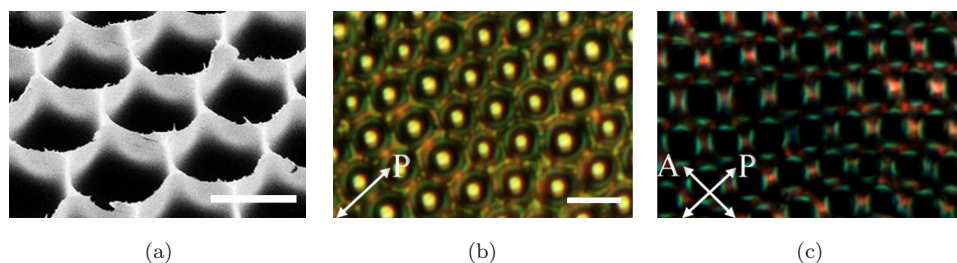


Fig. 6. (a) SEM of the peeled polymer film formed by breath figure templated self-assembly used as the base for atomic layer deposition (ALD). (b) Optical micrograph of ALD-coated polymer microbowls, showing a strong yellow reflection from the center of each bowl. (c) Optical micrograph with crossed polarizers, showing blue–green reflection from edges of bowls. (The red reflections between bowls are due to imperfect edges of peeled microbowls).



properties of the *P. palinurus* butterfly were replicated exactly. Comparisons of the CIE color curves for *P. palinurus* with the colors obtained from the physical emulation or mimicked structure were made. The color coordinates for the mimicry are somewhat less than for the butterfly, but fall within the end points of those measured for the butterfly, thus clearly demonstrating that with little refinement to these processes an exact copy can be obtained.

#### 4. *Princeps nireus*-Inspired Designs

Among all the coloration schemes so far identified in Lepidoptera, the “decorated” areas of the *Princeps nireus* butterfly demonstrate an astonishing variety of optical effects: absorption, photoluminescence, a 2D photonic crystal filter in the plane of the wing and, perpendicular to this, a Bragg reflector (first documented by Vukusic *et al.*<sup>14</sup>). The details of these various mechanisms are shown in Fig. 7. The green emission at 505 nm is attributed to a pigment infused into the wing section that is excited by blue skylight at 420 nm. SEM studies have shown that the wing consists of a hexagonal array of cuticle and that beneath this a triple-layer

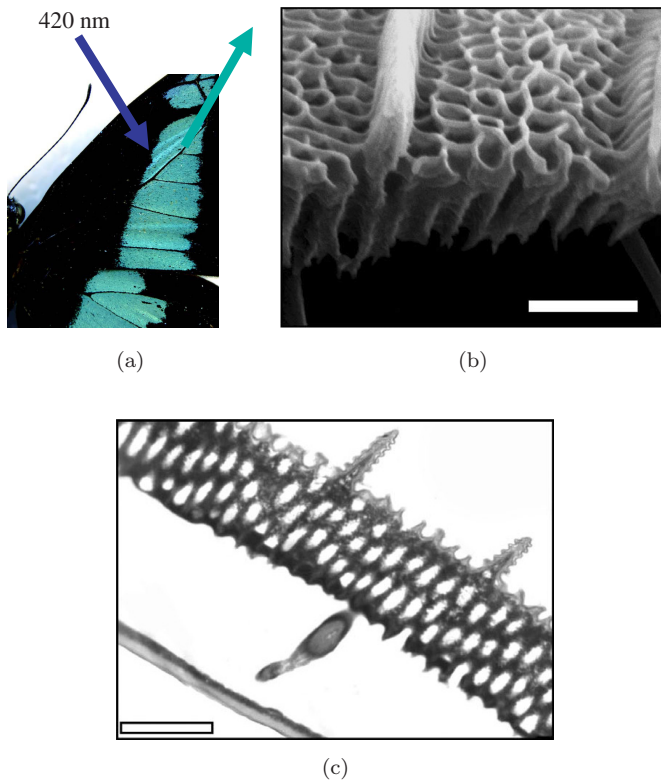


Fig. 7. *P. nireus* butterfly: (a) fluorescent wing section; (b) SEM of cuticle structure, showing a quasi-hexagonal structure; (c) TEM cross-section of cuticle and Bragg reflector.<sup>14</sup>

Bragg reflector. From these structure characterizations and optical simulations, the 2D PC structure is projected to have a photonic band gap at  $\sim 505\text{ nm}$ , and similarly the Bragg reflector reflects light in the same spectral bandwidth. Thus, the emission from the pigment is inhibited from propagating along the plane of the wing and, when propagated into the wing, is reflected by the Bragg reflector to exit the structure from the top surface. This strategy intensifies the emission of  $505\text{ nm}$  light perpendicular to the wing and is reported to increase the visibility of the butterfly by an order of magnitude.

We propose that this bioinspired strategy for controlling light can have significant applications in the detection of radiation — as, for example, required in scintillator crystals. Scintillators designed for the detection of gamma rays and neutrons are large (typically cylinders of  $5\text{ cm}$  diameter and  $5\text{ cm}$  length) because of the extended interaction lengths involved and light is generated at random points and emitted in random directions. Typically, the scintillated light undergoes 12–14 reflections before being focused into a detector. Thus, efficient light collection is a challenge, and a mechanism whereby light generation and its directionality could be controlled offers many advantages. Ideally, a full 3D photonic crystal structure could be designed to accomplish this degree of control and to enhance the efficiency of luminescence. However, the large volume required for scintillator action makes the fabrication of effective nanostructures a formidable task. The *P. nireus* strategy offers an alternative fabrication approach and demonstrates that the combination of a 2D + 1D photonic crystals offers a practical approach to controlling the direction of emitted light. Fortunately, several self-assembly techniques for the fabrication of fairly-large-area ( $>25\text{ cm}^2$ ) nanodimensional hexagonal lattice structures have been demonstrated. Large-scale opal formation has been reported by Wong *et al.*<sup>15</sup> and hexagonal “organ pipe” nanoscale arrays have been formed by electrochemical etching in silicon.<sup>16,17</sup> Using this technique, pure 2D PC hexagonal lattices (extended along the axis) can be formed and, as shown in Fig. 8, used to fabricate a PC scintillator. For scintillator applications high transparency is required in the visible. This can be obtained by thermally converting the Si template into  $\text{SiO}_2$ .

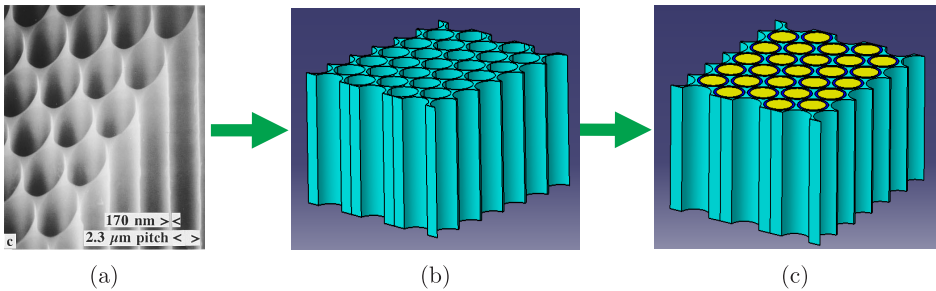


Fig. 8. (a) Example of a template from  $\text{SiO}_2$  (or  $\text{Al}_2\text{O}_3$ ), using electrochemical etching to form porous structure.<sup>16,17</sup> (b) Conformally coating with high-index material by ALD. (c) Infiltrating pores with scintillator material: anthracene, stilbene;  $n = 1.48$ ; scintillates at  $\sim 415\text{ nm}$ .

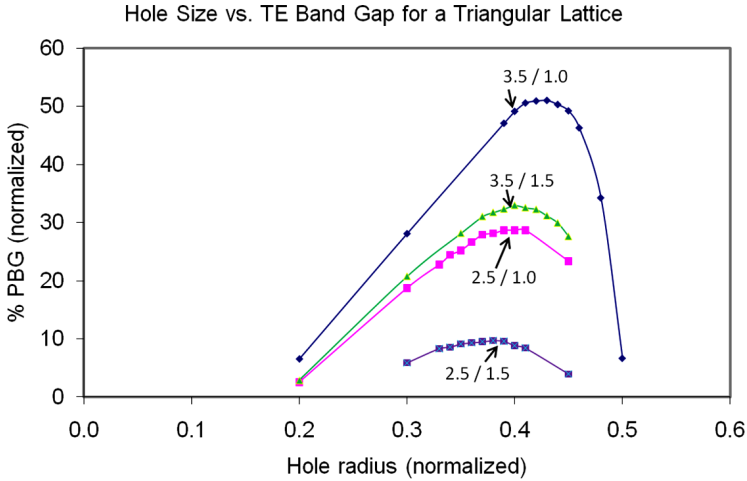


Fig. 9. Calculations of the PBG as a function of dielectric contrast and hole size for the TE mode triangular lattice.

(A similar technique has been used to form structures in alumina.) However, now the dielectric contrast between the PC lattice material and air is small, and so it is proposed to enhance the dielectric contrast by using ALD to conformally coat these low-index templates with a high-dielectric material, such as GaP or  $Zr_3N_4$  ( $n \sim 3.3$ ). The air cylinders are then filled with anthracene or stilbene, both of which have a low refractive index of  $\sim 1.46$  and are highly sensitive to gamma ray radiation and luminescence in the blue at  $\sim 420$  nm. Calculations of the photonic band structure are shown in Fig. 9. They predict a significant band gap of  $\sim 15\%$  for radiation polarized parallel to the PC. Thus, it is possible to inhibit a significant amount of radiation from propagating perpendicular to the axis of the structure, thereby enhancing emission along the longitudinal axis and the collection efficiency of scintillator radiation. Also, more complex structures could be designed which allow only one polarization mode to be generated and propagate, or which bring into coincidence the PBGs for the TE and TM modes, such as the annular photonic crystal.<sup>18</sup> Furthermore, placing a Bragg reflector or mirror at the end of the structure will reflect more radiation toward the detector. By making smaller structures and stacking them in a pixilated array, new scintillator designs can evolve that can be used to enhance detector sensitivity and potentially provide more information, such as the directionality of the incoming radiation source. Additional designs can involve the use of pillar arrays enclosed or immersed within the scintillator material.

## 5. Summary

In the first investigation, the unique use of structural color and optical properties of butterflies were investigated and employed to inspire new designs. Intact and broken scales of the *Papilio blumei* butterfly were conformally infiltrated by

low-temperature atomic layer deposition (ALD) of TiO<sub>2</sub>, resulting in distinct multicolor optical behavior. The modifications of the reflectance spectrum due to the deposition of highly conformal coatings were found to be in good agreement with theoretical data despite the simplicity of the model. Our approach demonstrates the potential not only to tune the reflectance and transmittance properties of complex photonic crystal templates encountered in Nature but also to produce high-index replicas with unique properties. Finally, we note that the results of this study provide a deeper understanding of the structural complexity of the butterfly scale architecture.

Precise mimicry of the structure and color properties of the *P. palinurus* butterfly was achieved using breath figure self-assembly and multilayer ALD. Good control over color was attained. Other approaches can also be considered, such as the formation of hexagonal arrays by nanoparticle (silica) self-assembly.

Consideration of the structure and properties of the *P. Nireus* wing structure has inspired new designs for radiation scintillator detectors by demonstrating that a two-component, 2D PC + 1D PC (PC plus Bragg reflector), optical system can fully address this application and provide a simpler approach than trying to fabricate a full 3D photonic crystal. Also, the structure can be fabricated by self-assembly techniques such as electrochemical etching followed by ALD, and infiltration of higher-index material, before being infiltrated with a liquid scintillator material.

The studies highlight the fact that Nature continues to be a source of inspiration in many unexpected ways by offering alternative routes for fabrication and designing bioinspired materials/devices with unique optical properties.

## Acknowledgment

M.S. and J.O.P. would like to acknowledge support from the National Science Foundation through grant DMR-0907529.

## References

1. M. Srinivasarao, Nano-optics in the biological world: Beetles, butterflies, birds and moths, *Chem. Rev.* **99** (1999) 1935.
2. S. Kinoshita and S. Yoshioka, *Structural Colors in Biological Systems: Principles and Applications* (Osaka University Press, Osaka, 2005).
3. R. W. Burnham, R. M. Hanes and C. J. Bartleson, *Color* (Wiley, New York, 1963).
4. P. Vukusic, R. Sambles, C. Lawrence *et al.*, Sculpted-multilayer optical effects in two species of Papilio butterfly, *Appl. Opt.* **40** (2001) 1116.
5. H. Tada, S. E. Mann, I. N. Miaoulis *et al.*, Effects of a butterfly scale microstructure on the iridescent color observed at different angles, *Opt. Exp.* **5** (1999) 87.
6. P. Vukusic, J. R. Sambles and C. R. Lawrence, Structural colour: Colour mixing in wing scales of a butterfly, *Nature* **404** (2000) 457.
7. J. S. King, E. Graugnard and C. J. Summers, Photonic crystals fabricated using patterned nanorod arrays, *Adv. Mat.* **17** (2005) 1010.
8. N. Otha and A. R. Robertson, *Colorimetry: Fundamentals and Applications* (John Wiley & Sons, Chichester, 2005).

9. V. Welch, V. Lousse, O. Deparis *et al.*, Orange reflection from a three-dimensional photonic crystal in the scales of the weevil *Pachyrrhynchus congestus pavonius* (curculionidae), *Phys. Rev. E* **75** (2007) 041919.
10. D. P. Gaillot, O. Deparis, B. K. Wagner, V. Welch, J. P. Vigneron and C. J. Summers, Composite organic-inorganic butterfly scales: Production of photonic structures with atomic layer deposition, *Phys. Rev. E* **78** (2008) 031922.
11. J. Huang, X. Wang and Z. L. Wang, Controlled replication of butterfly wings for achieving tunable photonic properties, *Nano Lett.* **6** (2006) 2325.
12. F. Garcia-Santamaria, M. Ibisate, I. Rodriguez *et al.*, Photonic band engineering in opals by growth of Si/Ge multilayer shells, *Adv. Mater.* **15** (2003) 788.
13. J. S. King, E. Graunard, O. M. Roche *et al.*, Infiltration and inversion of holographically defined polymer photonic crystal templates by atomic layer deposition, *Adv. Mater.* **18** (2006) 1561.
14. P. Vukusic and I. Hooper, Directly controlled fluorescence emission in butterflies, *Science* **310** (2005) 1151.
15. S. Wong, V. Kitaev and G. A. Ozin, Colloidal crystal films: Advances in universality and perfection, *J. Am. Chem. Soc.* **125** (2003) 15589.
16. M.-L. Zhang, K.-Q. Peng, X. Fan *et al.*, Preparation of large-area uniform silicon nanowires arrays through metal-assisted chemical etching, *J. Phys. Chem. C* **112** (2008) 4444.
17. U. Grüning, V. Lehmann, S. Ottow and K. Busch, Macroporous silicon with a complete two-dimensional photonic band gap centered at  $5\mu\text{m}$ , *Appl. Phys. Lett.* **68** (1996) 747.
18. H. Kurt and D. Citrin, Annular photonic crystals, *Opt. Exp.* **13** (2005) 10316.